Biogeochemical properties of the Ross Sea retrieved from in situ and remote optoelectronics devices during the Austral summer 1997-98.

JOURNAL OF OPTOELECTRONICS AND ADVANCED MATERIALS Vol. 8, No. 4, August 2006, p. 1565 - 1573

Biogeochemical properties of the Ross Sea retrieved from *in situ* and remote optoelectronics devices during the Austral summer 1997-98

R. BARBINI, M. CABRINI[a], F.COLAO, R. FANTONI, L. FIORANI[*], S. FONDA UMANI[a], N. V. KOLODIKOVA[b], L. LAZZARA[c], A. PALUCCI, F. PARMIGGIANI[d]
Sezione Applicazioni Laser – ENEA, Via Fermi 45, 00044 Frascati, Italy
[a]Laboratorio di Biologia Marina, Via Piccard 54, 34010 Trieste, Italy
[b]Tomsk State University of control Systems and Radioelectronics, Lenin Avenue 40, 634050 Tomsk, Russia
[c]Dipartimento di Biologia Animale e Genetica – Università di Firenze, Via Pieraccini 6, 50125 Firenze, Italy
[d]Istituto di Scienze dell'Atmosfera e del Clima – CNR, Via Gobetti 101, 40129 Bologna, Italy

The Southern Ocean and, in particular, the Ross Sea are among the more productive water bodies of the world ocean. The great impact of primary production on the global carbon cycle and, consequently, on the future climate justifies the large efforts devoted to its accurate assessment. In this paper, we present the results obtained with *in situ* optical methods (phytoplankton composition and pigment recognition), an active remote sensor (lidar fluorosensor) and passive remote sensors (satellite radiometers), in the framework of the 13th Italian Antarctic Oceanographic Campaign (December 1997 – January 1998). The synoptic picture gained by the integration of those different optoelectronics devices reveal interesting features of the phytoplankton blooms taking place in the Ross Sea during the Austral summer 1997-98. In particular, our primary production data are higher than previous estimates.

(Received June 27, 2006; accepted July 20, 2006)

Keywords: Lamp spectrofluorometer, Lidar fluorosensor, Satellite radiometer, Phytoplankton, Antarctica

1. Introduction

Scientific investigations in the Southern Ocean, mainly in the western Ross Sea, are part of the Italian Antarctic Research Program (PNRA), carried out during short- and long-term experiments in the framework of different projects (RossMIZE, CLIMA etc.). These surveys are performed in order to supply information on physical, chemical and biological processes affecting the investigated area, where a high spatial and temporal variability has prevented reliable, accurate and comprehensive estimates of the contribution to the carbon cycle of the Southern Ocean and, consequently, of its importance as a food source for higher trophic levels.

In general, the Antarctic seawaters are characterized by high turbidity, low salinity and high nutrient concentration. This latter is responsible for the growth of natural phytoplankton during the period of intense solar illumination (Lazzara *et al.*, 2000).

Among the water bodies surrounding Antarctica, Ross Sea is one of the most productive continental shelf system experiencing one of the most predictable and spatially expansive phytoplankton bloom in all the Southern Ocean (Comiso *et al.*, 1993; Arrigo and McClain 1994; Arrigo *et al.*, 2000; Smith *et al.*, 2000). The Ross Sea high production plays a relevant role in the downward carbon flux. The magnitude of the flux however depends on the food web structure. Primary production may be respired within the euphotic layer or can be channeled by vertical export of sinking materials and/or through the biomass of larger consumers. The flux of biogenic carbon towards large metazoans (i.e. renewable resources) and into deep waters (i.e. carbon sequestration) plays a pivot role for regulating the concentration of atmospheric CO_2 and is nowadays a matter of great concern. Primary production by pico- to micro-plankton is the base of the trophic web towards zooplankton, fishes, whales, seals and birds. Two phytoplankton taxa dominate the phytoplankton assemblage of the region: diatoms, which often occur in the western and eastern portions of the southern Ross Sea (see e.g. Sweeney *et al.*, 2000) and prymnesiophytes (i.e. *Phaeocystis antarctica*), which generally are found in the open polynya of the western and south-central region (Di Tullio and Smith, 1996; Arrigo *et al.*, 1999; Dennett *et al.*, 2001). In general, the distribution patterns of *Phaeocystis antarctica* and diatoms were found non-overlapping (but not mutually exclusive) in the Ross Sea (Arrigo *et al.*, 1999; Smith and Asper, 2001).

Humic substances are known to play a major role in many biogeochemical processes taking place in coastal and offshore waters, including transportation and speciation of trace metals (Mantoura *et al.*, 1978). In the Antarctic area, most of the inorganic particulate, released after ice melting, is complexed by humic substances, thus contributing to increase the phytoplankton productivity. In contrast, the Southern Ocean from the lower latitudes up to the Antarctic Convergence, collects impurities from the entire hemisphere and is characterized by strong mixing effects with water masses surrounding Antarctica (Circumpolar Current). The study of the hydrological and

biological seawater parameters in these areas is important for a better understanding of the interactions with the surrounding environment, including the atmospheric CO_2 uptake (Tréguer and Jacques, 1992; JGOFS, 2003), which in turn drive the climatic evolution of the planet.

Ocean color satellite images (Joint and Groom, 2000) have proven to be powerful tools in giving a synoptic view of the phytoplankton dynamics in the Southern Ocean. Nevertheless, their estimates of primary production in Antarctic surface seawaters should be taken with care: e.g. Arrigo *et al.* (1998) found a value of 4.4 Tg C yr^{-1}, 4-5 times higher than previous estimates, made from extrapolated ^{14}C measurements. This could be in part ascribed to the persistent cloud coverage that makes it difficult to get continuous imagery from space. The development of new algorithms, able to track the seasonal and yearly variability of primary production in the regional or larger scale, requires an improvement in accuracy and coverage of the chlorophyll measurements in the Ross Sea polynya and in the offshore waters of the Southern Ocean. This aim can be achieved by means of *in situ* standard techniques as well as data from active and passive remote sensors.

In this paper, after a description of instruments and methods, a biogeochemical characterization of the Ross Sea during the Austral summer 1997-98 is given. In particular, the chlorophyll-a (Chl-a) and Colored Dissolved Organic Matter (CDOM) data, gathered by the ENEA lidar fluorosensor (ELF) (Barbini *et al.*, 2001a) during the 13th Italian Antarctic Oceanographic Campaign (December 1997 – January 1998), are both used to improve the satellite estimates of primary production and to describe the optical properties of the investigated waters.

1. Instruments and methods

1.1. Sea-ice and Sea Surface Temperature (SST) maps

The family of polar orbiting environmental satellites from NOAA-6 to NOAA-15 mounts on board the Advanced Very High Resolution Radiometer (AVHRR) (Thomas *et al.*, 1989) which operates in five spectral channels: visible (channel 1), near-infrared (channel 2) and thermal infrared (channels 3 – 5).

Raw AVHRR data covering the whole Ross Sea were acquired by the NOAA receiving station installed at the Italian base at Terra Nova Bay (TNB). AVHRR data processing consists of the following steps:

1. Calibration. The solar channels 1 and 2 are calibrated into % technical albedo as described by the NOAA manual. The thermal infrared data are converted from raw counts to radiances with a linear relationship based on the raw count value associated with the cold space and the raw count value associated with the temperature of an onboard blackbody. A slight nonlinearity in channels 4 and 5 is corrected using a quadric function of radiance. Lastly, the infrared radiances are converted to brightness temperatures (°C) using the inverse Planck function, i.e. they are derived via a temperature-radiance look-up table.
2. Cloud Screening and Clearing. To ensure that SST values are derived only for cloud free water surfaces, two cloud tests are performed. They are based on the principal characteristics of water bodies, considering the typical spectral and textural parameters characterizing their dark, warm, and homogenous surface. All pixels which are flagged as "CLOUD" or "NO SST" are excluded from all further processing.
3. Multichannel Sea Surface Temperature (MCSST). The applied formula is based on the brightness temperatures of AVHRR channels 4 and 5 (T4, T5) and is described by McClain *et al.* (1985). This technique is known as the "Split Window Technique" and corrects atmospheric attenuation mainly caused by the water vapor absorption in the atmosphere: if not accounted for, this absorption can lead to a significant drop in derived brightness temperatures and thus to a significant error in SST computation.
4. Composite SST maps. In order to reduce cloud cover, composite SST maps are produced by means of several MCSST images composed together by taking the maximum temperature value at every pixel position.

Steps 1 to 4 are performed by means of specific commands of the commercial software package TeraScan (by SeaSpace Corp., Poway, California) in use both at CNR and at TNB.

AVHRR channel 2 images are often used to obtain a picture of the sea ice coverage (like in Fig. 1) while the most important use of AVHRR is to produce SST maps (like in Fig. 2).

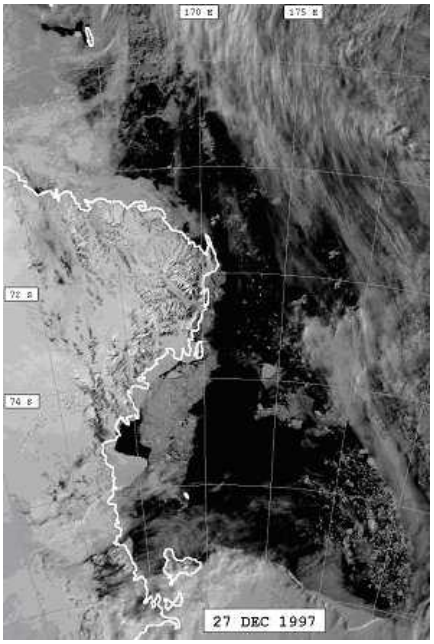

Fig. 1. Satellite derived image of ice distribution in the western Ross Sea area [AVHRR, December 27, 1997].

1.2. Satellite maps of Chl-a concentration

Regional maps of Chl-a concentration can be obtained from satellite imagery thanks to atmospheric corrections (Fiorani *et al.*, 1998) and bio-optical algorithms (O'Reilly *et al.*, 1998). Firstly, the water-leaving radiance is calculated with the atmospheric corrections that remove from the sensor measurements the contributions of air molecules and aerosols. Secondly, the Chl-a concentration is retrieved from the water-leaving radiances in the visible bands with a set of empirical equations named bio-optical algorithms (Fig. 3). If the data are calibrated through *in situ* measurements, we can obtain quantitative estimations of Chl-a concentrations within the surface layer of a given water body.

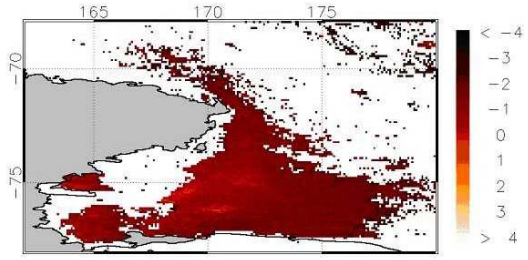

Fig. 2. Composite SST map of the western Ross Sea [AVHRR, December 19 to 26, 1997]. The color code refers to temperatures in °C.

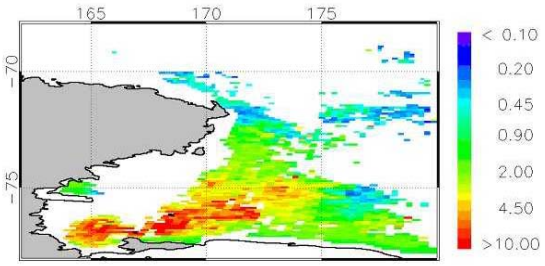

Fig. 3. Satellite Chl-a concentration in the western Ross Sea [SeaWiFS, December 19 to 26, 1997]. The color code refers to concentrations in mg/m^3.

The first observations of ocean color from space were carried out by the Coastal Zone Color Scanner (CZCS) (Hovis, 1980), which operated on board the Nimbus-7 satellite from 1978 to 1986. The Sea-viewing Wide Field-of-view Sensor (SeaWiFS) (Hooker *et al.*, 1992) can be considered the follow-on sensor to CZCS. It was launched on August 1, 1997 on board the OrbView-2 satellite and started data acquisition on September 4, 1997. SeaWiFS operates with 8 channels in the visible and near-IR range of the electromagnetic spectrum; it is expected to greatly improve our understanding of the oceanic processes as its accuracy resulted better than 35% for Chl-a concentration over the range of 0.05-50 mg m^{-3}.

1.3. In situ phytoplankton composition

In order to investigate the *in situ* phytoplankton composition, samples of 500 ml were preserved with buffered formalin (final concentration: 4%) and stored in dark glass bottles. Phytoplankton identity and abundance were determined on 50-ml aliquots with an inverted microscope according to the Uthermohl method as described by Zingone *et al.* (1990). For the identification of species the main taxonomy references were used (Priddle and Fryxell, 1985; Medlin and Priddle, 1990; Throndsen, 1993; Hasle and Syvertsen, 1996; Steindinger, 1996). Analyses were carried out on 117 samples collected during the 13th Italian Antarctic Oceanographic Campaign. The samples were taken both at the sea surface and at different depths in stations located in the TNB polynya, along the Drygalsky Ice Tongue, in the Ross Ice Shelf (RIS) and in the open Ross Sea.

1. 4. Spectroscopic phytoplankton pigment recognition

A lamp spectrofluorometer (PTI Quantamaster) has been used to collect excitation and emission spectra from unfiltered water samples picked up every hour, both from the sea surface and 5 m underneath. The instrument was employed to obtain reference fluorescence emission spectra, to be compared with the *in situ* sea water analysis and finally to calibrate ELF remote data (Barbini *et al.*, 2001b). In this case, fluorescence spectra were processed starting with a background subtraction, and proceeding through a multiple Gaussian deconvolution of unresolved or overlapped structures. Resolved peaks were then integrated within a 10 nm bandwidth and normalized to the relevant water Raman peak.

Moreover, excitation spectra were also performed, in order discriminate and to follow changes in pigment composition along the route. As an example, excitation spectra (λ_{em}=680 nm) for seawater samples collected in the TNB area is depicted in Fig. 4. The contributions of Chl-a (430 nm), Chl-c (460 nm), Chl-b (480 nm), carotenoids (380 and 520 nm) and phaeopigments (410, 505 and 590 nm) can be found at the spectral wavelengths marked by the arrows.

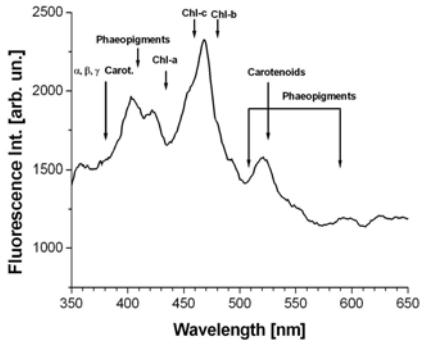

Fig. 4. Excitation spectra at the hydrographic station 4 of Table 1 [λ_{em}=680 nm].

1.5. ELF Chl-a concentration

ELF (Barbini *et al.*, 2001a) is an optical radar (Measures, 1992), based on Laser-Induced Fluorescence (LIF) and LIght Detection And Ranging (lidar). It has been developed in the framework of PNRA for oceanographic campaigns aboard the research vessel (RV) *Italica*.

The main components of the light source are a frequency-tripled Q-switched Nd:YAG laser and a beam expander. Usually, the operational parameters are: wavelength = 355 nm, pulse duration = 10 ns, pulse energy = 10 mJ and repetition rate = 10 Hz. ELF transmits the exciting beam and receives the generated radiation through an optical window and a flat mirror in order to reach the water surface at normal incidence. The optical signal, after collection by a telescope, crosses a dichroic mirror (rejection of the light backscattered at 355 nm) and is then directed through a fiber bundle to 4 interference filters (spectral selection) and thereof falls on photomultiplier tubes (detection). The 4 optical channels have a full width at half maximum (FWHM) of 5 nm and correspond to Raman scattering of water (404 nm), fluorescence of CDOM (450 nm), phycoerythrin (585 nm) and Chl-a (680 nm), respectively. The electronic output is digitized by analog-to-digital converters. A personal computer, embedded in a Versa Module Eurocard (VME) bus, controls all the operational parameters.

The beam footprint and penetration on the water body are of about 0.1 and 10 m, respectively. Usually the data are time integrated for 5 s. Taking into account the average speed of the RV, each data point taken by ELF correspond to an approximately 0.1 m wide, 12 m long and 10 m deep track. At first, fluorescence signals are released in Raman units, i.e. they are normalized to the water Raman peak. Afterwards, they are converted into pigment concentrations by calibration against conventional analysis on the same water. During the 13th Italian Antarctic Oceanographic Campaign the Chl-a extractions were performed by De Vittor *et al.* (2000) according to the spectrofluorometric technique described by Lorenzen and Jeffrey (1980). The correlation coefficient between fluorescence signals and Chl-a extractions was 0.91 (Barbini *et al.*, 2001b).

After being processed and calibrated, Chl-a lidar concentrations have been reported upon a digital cartographic base to obtain a thematic map such as in Fig. 5, which represent an along-route color coded distribution.

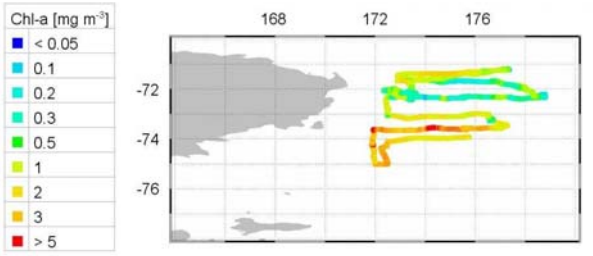

Fig. 5. Chl-a distribution measured with the lidar fluorosensor along the ship route [December 19 to 26, 1997].

In the case of CDOM, the fluorescence data are released in Raman units.

1.6. ELF-tuned primary production

As mentioned before, the data processing used to obtain regional maps of Chl-a concentration from space imagery has to be tuned through *in situ* measurements. Unfortunately, these latter are quite rare in the Southern Ocean (O'Reilly *et al.*, 1998). Probably, this is the main reason of the underestimation of primary production observed in Antarctic waters (Arrigo *et al.*, 1998). In order to refine the satellite estimate, the SeaWiFS bio-optical algorithm has been calibrated in the Ross Sea on the basis of the ELF Chl-a data acquired during the 13th Italian Antarctic Oceanographic Campaign, as explained by Barbini *et al.* (2003). As expected, the values given by the ELF-calibrated bio-optical algorithms are higher than the standard SeaWiFS Chl-a concentration (average percent difference of about 20%).

Once the corrected Chl-a concentration has been obtained with the ELF-calibrated bio-optical algorithm, it can be used for the calculation of the phytoplankton primary production. For this purpose, the simple model (Falkowski *et al.*, 1998)

$$\log_{10} \Sigma PP = 2.793 + 0.559 \log_{10} C \qquad (1)$$

where ΣPP is the daily depth-integrated primary production in mgC m^{-2} d^{-1} and C the Chl-a concentration in mg m^{-3}, has been chosen because it represents a sort of consensus algorithm for SeaWiFS and, as described elsewhere (Barbini *et al.*, 2003), its values are close to the average of two recent and refined models (Behrenfeld and Falkowski, 1997; Dierssen *et al.*, 2000), at least in the Ross Sea during the Austral summer 1997-98. In this latter case, the estimated accuracy of ΣPP is about 65% (Barbini *et al.*, 2003).

1.7. ELF-tuned CDOM absorption coefficient

The retrieval of the CDOM concentration from satellite imagery is a difficult task. A preliminary algorithm has been suggested by Aiken *et al.* (1995). More recently, an empirical algorithm (Miller *et al.*, 2000) and a semi-analytical algorithm (Siegel *et al.*, 2002) have been developed in order to obtain the CDOM absorption coefficient at a given wavelength. The empirical algorithm is expressed by

$$\log_{10}\left[a_{CDOM}(355)\right] = a_0 + a_1 \log_{10}\left[\frac{Rrs(412)}{Rrs(555)}\right], \qquad (2)$$

where $a_{CDOM}(355)$ is the CDOM absorption coefficient at 355 nm, Rrs(412) and Rrs(555) are the remote sensing reflectances measured by SeaWiFS at 412 nm and 555 nm, respectively, and has the advantage to be easily tunable with the large amount of *in situ* data provided by ELF. In

fact, according to Hoge *et al.* (1995) the CDOM absorption coefficient at 355 is given by

$$a_{CDOM} = 0.049 + 1.28\frac{F_{450}}{R_{404}} \quad (3)$$

where F_{450} and R_{404} are the CDOM fluorescence and Raman scattering signals measured at 450 nm and 404 nm, respectively. The calibration of the empirical algorithm is the result of the linear fit of $\log_{10}[a_{CDOM}(355)]$, determined by ELF, versus $\log_{10}$[Rrs(412)/Rrs(555)], obtained by SeaWiFS, when the acquisition space and time of ELF was contained in the space interval and time period of the corresponding SeaWiFS pixel. An example of the retrieval of $a_{CDOM}(355)$ is given in Fig. 6.

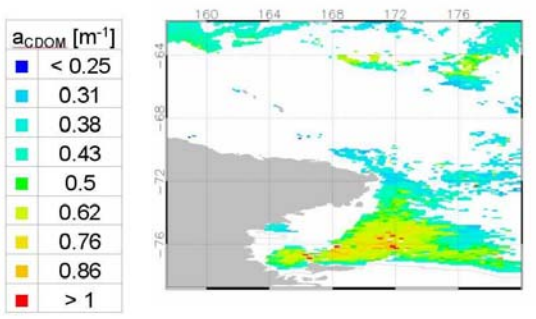

Fig. 6. ELF-tuned satellite CDOM concentration in the Ross Sea [SeaWiFS, December 19 to 26, 1997].

2. Biogeochemical properties of the Ross Sea

Widely different seawaters masses have been monitored during the oceanographic campaign, ranging from offshore oceanic to inshore or polynya areas, due to the favorable environmental conditions met during the Austral summer 1997-98.

The presence of icebergs and pack were limited to few occurrences a part from a belt around the TNB polynya, thus resulting free seawater surface in most part of the Ross Sea, as can be observed from the satellite frame of Fig. 1. Moreover, the season was characterized by a constant high solar radiation on the open sea, with an average Photosynthetically Active Radiation (PAR) of 280 μmol m^{-2} s^{-1}, thus resulting in a constant and uniform superficial temperature (Fig. 2), in the range of 0÷-2 °C.

The continuous lidar monitoring and the sampling activity on board of the RV *Italica*, was largely extended in the present campaign, but we focus our attention to the superficial components at nine hydrographic stations. Details of the phytoplankton characterization are reported in Table 1, while their geographical position is shown in Fig. 7.

Table 1. Superficial phytoplankton composition and biomass concentration at different stations in the western Ross Sea.

Zone	Station	Latitude	Longitude	Date	Species	Concentration [cell/l]	Concentration [%]
TNB	4	75 12'.14 S	163 59'.95 E	12/08/97	Phaeocystis	1 340 000	98.3
Drygalsky	69	75 21'.16 S	164 56'.10 E	01/26/98	Fragilariopsis	84 720	98.1
Drygalsky	76	75 47'.36 S	165 27'.74 E	01/27/98	Fragilariopsis	50 880	80.4
Drygalsky	80	76 29'.91 S	163 59'.70 E	01/28/98	Fragilariopsis	71 600	54.4
RIS	103	76 49'.88 S	176 00'.44 E	02/02/98	Phaeocystis	1 320 000	96.3
RIS	107	76 49'.93 S	169 59'.74 E	02/03/98	Phaeocystis	400 000	44.1
RIS	112	76 19'.88 S	174 26'.92 E	02/04/98	Phaeocystis	3 520 000	87.2
TNB	148	74 49'.72 S	166 12'.69 E	02/12/98	Fragilariopsis	792 000	98.2

The phytoplankton structure in the TNB polynya, the Drygalsky basin and the RIS can be better analyzed if we distinguish the whole period in: 1) late spring, 2) early-mid summer and 3) late summer as suggested by Fonda Umani *et al.* (2002). In December 1997, a first *Phaeocystis* cfr. *antarctica* bloom is recorded in the TNB polynya, with the occurrence of both individual cells and colonies (Station 4). The concentration reaches 1.5×10^6 cell/l at the surface and in the upper 50 m. This small prymnesyiophycaea is the dominant species and is responsible of early spring and late summer blooms in the open polynya of the western and southern central Ross Sea (Di Tullio and Smith, 1996; Marino and Cabrini, 1997; Arrigo *et al.*, 1999; Dennett *et al.*, 2001). In January, after the ice melting, diatoms represent the dominant autotrophic fraction. The most abundant species along the Drygalsky Ice Tongue (Stations 69, 76 and 80) were *Fragilariopsis cylindrus*, *Fragilariopsis curta* and *Fragilariopsis kerguelensis* (Cabrini and Cataletto, 2000). Their occurrence gradually decreases in the coastal stations along the RIS in the upper 100 m, while *Phaeocystis* cfr. *antarctica* was completely absent. In the community other diatoms (e.g. *Actinocyclus actinochilus*, *Stellarima microtrias*, *Asteromphalus hookeri*, *Corethron criophilum*, *Chaetoceros dichaeta*) and other undetermined nanoflagellates are found in low densities

(always <50000 cell/l). In early February (3-7) 1998, all along the RIS, a widespread bloom of *Phaeocysts* cfr. *antarctica* is registered at the surface (Stations 103, 107 and 112), with the maximum of 3.5×10^6 cell/l at station 112. Few diatoms, nanoflagellates and dinoflagellates are also observed. In the late summer (end of February), in the TNB polynya, the diatom community prevails in the upper 100 m and presents the highest specific diversity (Station 148). Nevertheless, *Fragilariopsis cylindrus*, *Fragilariopsis curta*, *Fragilariopsis kerguelensis*, *Pseudonitzschia subcurvata* and *Pseudonitzschia pseudodelicatissima* represent the most abundant species in all the stations.

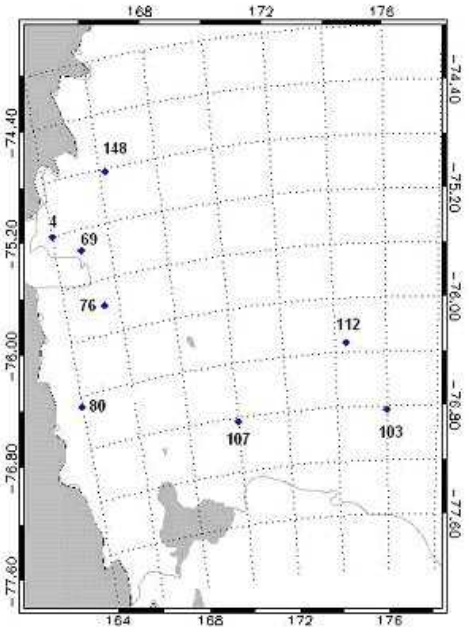

Fig. 7. Geographic map of the western Ross Sea. The main sampling sites are indicated, as reported in Table 1.

Excitation spectra collected during the cruise along the Southern Ocean down to TNB are reported in Fig. 8, almost at increments of 5 of latitude. Changes of pigment compositions of the crossed seawaters become evident by looking at spectra in sequence. Namely, the spectrum at 50 S (and to a minor extent the spectrum at 70 S) appears to be the most structured of the whole ensemble, due to the presence of all the Chl bands and of carotenoids, which corresponds to a mixed phytoplankton population. On the other hand, the spectrum at 55 S seems to be dominated by a diatom-like phytoplankton, with a lacking of the Chl-b band, while the spectrum at 65 S does not present the Chl-c feature but is dominated by Chl-a and Chl-b, as expected in the case of the *chlorophytes*. The spectrum at 75 S is dominated by Chl-c excitation, with a second peculiar peak at 520 nm, which can be attributed to *xanthophylls* excitation, both features supporting the presence there of a *Phaeocystis*-dominated phytoplankton as for station 4.

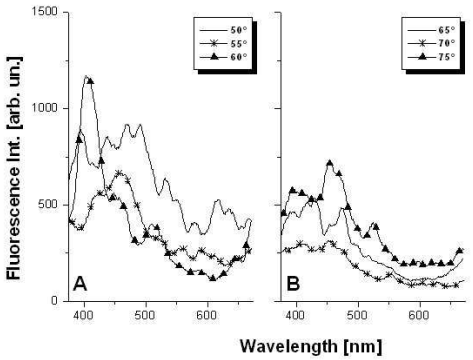

Fig. 8. Excitation spectra of the seawater crossed in the Southern Ocean: a) 50.91 S 172.88 E [25/11/97]; 54.95 S 173.16 E [26/11/97]; 60.36 S 175.6 E [27/11/97]; and in the Ross Sea: b) 65.0 S 179.17 E [28/11/97]; 70.51 S 179.01 E [30/11/97]; 74.99 S 169.48 E [01/12/97].

The ELF-tuned Chl-a algorithm has been applied to the 8-day L3 water-leaving radiances of SeaWiFS to obtain corrected primary productions in the western Ross Sea during the whole observation period. A phytoplankton bloom is seen to arise at a location northeast of the Ross Island in the period December 3 to 10, 1997, reaching its maximum concentration and spatial extent in the period December 19 to 26, 1997. The bloom fills the open sea located northeast of the Ross Island (Fig. 3). While the main bloom decays, a minor delayed algal development takes place in TNB (75.86 S 164.19 E) and in the Northern area near Cape Adare (71.33 S 170.17 E). Primary production peaks during the period December 19 to 26, 1997, when the main phytoplankton bloom attains its maximum.

In order to compare the ELF-calibrated algorithm with literature data, the average primary production in the western Ross Sea (157.5 E – 180.0 E, 72.07 S – 78.75 S) and in a larger region of the Southern Ocean (157.5 E – 180.0 E, 61.875 S – 78.75 S) has been plotted for the Austral summer 1997-98 (Fig. 9). As expected, the most productive month for the largest area of the Southern Ocean is December. Conversely, for the Ross Sea, the highest mean value is reached in February. This seasonal feature, a late summer second bloom, corresponds to an observation that has already been made in the Ross Sea (Nelson *et al.*, 1996; Arrigo *et al.*, 1998) and has been pointed out as peculiar at TNB since the Austral summer 1987-88 (Innamorati *et al.*, 1990; Lazzara *et al.*, 2000). The study by Arrigo *et al.* (1998), probably the most accurate and comprehensive on the Southern Ocean, made a comparison of all available CZCS data (1978-86) with *in situ* measurements. In the Ross Sea values between 470 and 640 mgC m^{-2} d^{-1} have been found during the Austral summer (monthly averaged ΣPP for January, February and March). Our data range from 660 to 1100 mgC m^{-2} d^{-1} in the same period and the average value in the Ross Sea for the six months between October 1997 and March 1998 is about 700 mgC m^{-2} d^{-1} corresponding to a yearly average

of 350 mgC m^{-2} d^{-1}, quite a high value, even if compared with the recent values of 125 mgC m^{-2} d^{-1} given by Smith *et al.* (1996) and of 120-160 mgC m^{-2} d^{-1} provided by Arrigo *et al.* (1998). Nevertheless, these values are consistent with the high daily primary production obtained by *in situ* measurements in the whole western Ross Sea both in December 1989 (from 210 to 2544 mgC m^{-2} d^{-1}; Lazzara *et al.*, 2000) and from November to December 1994 (from 100 to 3000 mgC m^{-2} d^{-1}; Saggiomo *et al.*, 2000). Moreover, from a temporal data set at TNB, production values estimated during the austral summer 1989-90 give an average of 1390 mgC m^{-2} d^{-1} from December to February (Lazzara *et al.*, 2000) that gives 241 mgC m^{-2} d^{-1} on a yearly base.

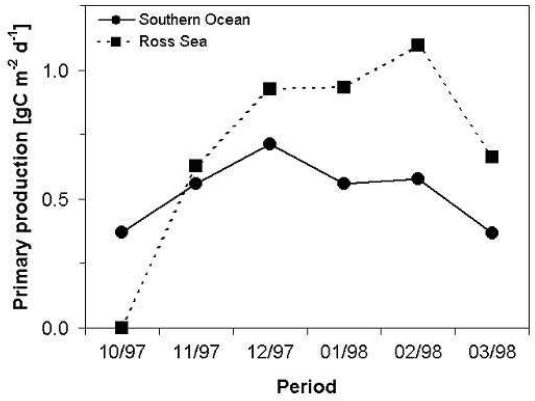

Fig. 9. Primary production based on ELF-calibrated SeaWiFS Chl-a concentration averaged in the Southern Ocean (157.5 E – 180.0 E, 61.875 S – 78.75 S) and in the Ross Sea (157.5 E – 180.0 E, 72.07 S – 78.75 S) during the Austral summer 1997-98.

The ELF-calibrated SeaWiFS algorithm for the CDOM absorption coefficient at 355 nm has been applied to the 8-day L3 products in the western Ross Sea during the whole observation period. The average $a_{CDOM}(355)$ in the western Ross Sea (157.5 E – 180.0 E, 72.07 S – 78.75 S) and in a larger region of the Southern Ocean (157.5 E – 180.0 E, 61.875 S – 78.75 S) has been calculated for the periods corresponding to six 8-day L3 SeaWiFS data products covering the 13th Italian Antarctic Oceanographic Campaign. A comparison with the primary production temporal dynamics in the same period shows a delay of 8 days of CDOM with respect to primary production, probably due to the senescence of the bloom with the increase of microbic degradation, lysis and also photo-oxidation, owing to the constantly elevated solar irradiance. As for the primary production, $a_{CDOM}(355)$ has been plotted monthly for the Austral summer 1997-98 (Fig. 10). The range of values we found compare well with the literature (Miller *et al.*, 2000). Recently, in a wide study on European coastal waters (North Sea included), Babin *et al.* (2003) found $a_{CDOM}(355)$ between 0.23 and 2.8 m^{-1}.

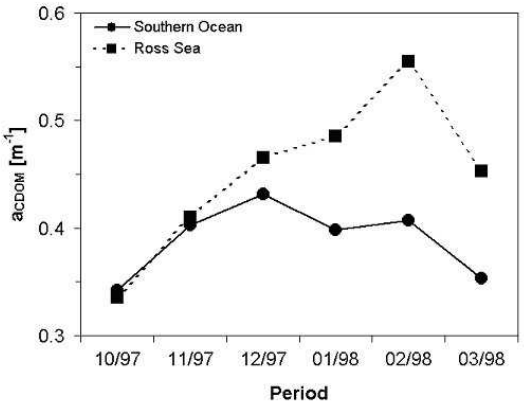

Fig. 10. CDOM absorption coefficient at 355 nm, based on the ELF-calibrated SeaWiFS algorithm, averaged in the Southern Ocean (157.5 E – 180.0 E, 61.875 S – 78.75 S) and in the Ross Sea (157.5 E – 180.0 E, 72.07 S – 78.75 S) during the Austral summer 1997-98.

The monthly average primary production and CDOM emission (Figs. 9 and 10), a part from a good correlation, has a clear seasonable behavior with maximum productivity in December and January and a marked increase in CDOM production in February.

3. Conclusions

The present merging among ground (*in situ*), lidar fluorosensor and satellite radiometer data resulted in a detailed description of the 1997-98 Austral summer, demonstrating how useful can be optoelectronics device in the environmental monitoring at various scales. The information gathered presents a pronounced primary production in the western Ross sea, compared to the Southern Ocean, with a strong influence of natural algal community in the polynya areas. A good correspondence between phytoplankton abundance collected *in situ* and lidar fluorosensor remote data was found.

The development of regional algorithms for satellite radiometers, based on calibrated *in situ* and remote lidar measurements can contribute to define new methodologies in remote sensing and *in situ* concepts. This task passes through a better definition of the optical properties (absorption and attenuation of the main components) as well as *in situ* reflectance and transmission of the seawater investigated that will be implemented in future campaigns.

Acknowledgements

This work has been supported by the Italian Antarctic Research Program (PNRA), Technology Sector, 5b1 Lidar Fluorosensor and 11-5 Palucc5 Projects (for the periods

1996-1998 and 1999-2001, respectively). The authors would like to thank the SeaWiFS Project (Code 970.2) and the Distributed Active Archive Center (Code 902) at the Goddard Space Flight Center, Greenbelt, MD 20771, for the production and distribution of these data, respectively. These activities are sponsored by NASA's Mission to Planet Earth Program.

References

[1] J. Aiken, G. F. Moore, C. C. Trees, S. B. Hooker, D. K. Clark, NASA Technical Memorandum 104566, Hooker, S. B., Firestone, E. R., eds. Greenbelt: NASA **29**, 34 (1995).

[2] K. R. Arrigo, G. R. Di Tullio, R. B. Dunbar, D. H. Robinson, M. Van Woert, D. L. Worthen, M. P. Lizotte, Journal of Geophysical Research C **105**, 8827 (2000).

[3] K. R. Arrigo, C. R. McClain, Science **266**, 261 (1994).

[4] K. R. Arrigo, D. H. Robinson, D. L. Worthen, R. B. Dunbar, G. R. Di Tullio, M. Van Woert, M. P. Lizotte, Science **283**, 365, (1999).

[5] K. R. Arrigo, D. Worthen, A. Schnell, M. P. Lizotte, Journal of Geophysical Research C **103**, 15587 (1998).

[6] R. Barbini, F. Colao, R. Fantoni, A. Palucci, S. Ribezzo, International Journal of Remote Sensing **22**, 369 (2001).

[7] M. Babin, D. Starmski, G. Ferrari, H. Claustre, A. Bricaud, G. Obolensky, N. Hoepffner, Journal of Geophysical Research C **108**, 3221 (2003).

[8] R. Barbini, F. Colao, R. Fantoni, L. Fiorani, A. Palucci, J. Optoelectron. Adv. Mater. **3**, 817 (2001).

[9] R. Barbini, F. Colao, R. Fantoni, L. Fiorani, A. Palucci, Antarctic Science **15**, 77 (2003).

[10] M. J. Behrenfeld, P. G. Falkowski, Limnology and Oceanography **42**, 1479 (1997).

[11] M. Cabrini, B. Cataletto, Fioritura di diatomee nel Mare di Ross nell'estate australe 1998. Atti dell'Associazione Italiana di Oceanologia e Limnologia **13**, 289 (2000).

[12] J. C. Comiso, C. R. Mc Clain, C. W. Sullivan, J. P. Ryan, C. L. Leonard, Journal of Geophysical Research C **98**, 2419 (1993).

[13] M. R. Dennet, S. Mathot, D. A. Caron, W. O. Smith Jr., D. J. Lonsdale, Deep-Sea Research II **48**, 4019 (2001).

[14] C. De Vittor, M. Cabrini, E. Crevatin, S. Fonda Umani, Atti dell'Associazione Italiana di Oceanologia e Limnologia **13**, 249 (2000).

[15] H. M. Dierssen, M. Vernet, R. C. Smith,. Optimizing models for remotely estimating primary production in Antarctic coastal waters. Antarctic Science **12**, 20 (2000).

[16] G. R. Di Tullio, W. O. Smith Jr., Journal of Geophysical Research C **101**, 18467 (1996).

[17] P. G. Falkowski, M. J. Behrenfeld, W. E. Esaias, W. Balch, J. W. Campbell, R. L. Iverson, D. A. Kiefer, A. Morel, J. A. Yoder, NASA Technical Memorandum 104566, Hooker, S. B., Firestone, E. R., eds. Greenbelt: NASA **42**, 36 (1998).

[18] L. Fiorani, S. Mattei, S. Vetrella, Laser methods for the atmospheric correction of marine radiance data sensed from satellite. Proceedings of SPIE **3496**, 176 (1998).

[19] S. Fonda Umani, A. Accornero, G. Budillon, M. Capello, S. Tucci, M. Cabrini, P. Del Negro, M. Monti, C. De Vittor, Particulate matter and plankton dynamics in the Ross Sea Polynya of Terra Nova Bay during the Austral Summer 1997/98. Journal of Marine Systems **36**, 29 2002

[20] G. R. Hasle, E. Syvertsen, Marine diatoms. In: Identifying Marine Diatoms and Dinoflagellates. Tomas, C. R., ed. San Diego: Academic Press, pp. 1, 1996.

[21] F. E. Hoge, A. Vodacek, R. N. Swift, J. K. Yungel, N. V. Blough, Inherent optical properties of the ocean: retrieval of the absorption coefficient of chromophoric dissolved organic matter from airborne laser spectral fluorescence measurements. Applied Optics **34**, 7032 (1995).

[22] S. B. Hooker, C. R. McClain, J. K. Firestone, T. L. Westphal, E-n. Yeh, Y. Ge,. The SeaWiFS Bio-Optical Archive and Storage System (SeaBASS), Part 1. SeaWiFS Technical Report Series - NASA Technical Memorandum 104566 - Hooker, S. B., Firestone, E. R., eds. Greenbelt: NASA **20**, 40 (1994).

[23] W. A. Hovis, Nimbus-7 coastal zone color scanner: system description and initial imagery. Science **210**, 60 (1980).

[24] M. Innamorati, G. Mori, L. Massi, L. Lazzara, C. Nuccio, Spatial and temporal variations of phytoplankton biomass related to evironmental factors in the Ross Sea. In: Ross Sea Ecology. Italiantartide Expeditions (1987-1995). Faranda, F., Guglielmo, L., Ianora, A., eds. Berlin, Sprinter-Verlag 216 (2000).

[25] JGOFS (Joint Global Ocean Flux Study) Final Open Science Conference "A Sea of Change: JGOFS Accomplishments and the Future of Ocean Biogeochemistry", May 5-8, 2003, Washington, DC, USA

[26] I. Joint, S. B. Groom,. Estimation of phytoplankton production from space: current status and future potential of satellite remote sensing. Journal of Experimental Marine Biology and Ecology **250**, 233 (2000).

[26] L. Lazzara, V. Saggiomo, M. Innamorati, O. Mangoni, L. Massi, G. Mori, C. Nuccio, Photosynthetic parameters, irradiance and production estimates in the western Ross Sea. In: Ross Sea Ecology. Italiantartide Expeditions (1987-1995). Faranda, F., Guglielmo, L., Ianora, A., eds. Berlin, Sprinter-Verlag, pp. 259-273, 2000.

[27] C. J. Lorenzen, S. Jeffrey, SCOR UNESCO Technical Papers in Marine Science **35**, 1 (1980).

[28] R. F. C. Mantoura, A. Dickson, J. P. Riley, Estuarine and Coastal Marine Science **6**, 378 (1978).
[29] D. Marino, M. Cabrini, in: RossMIZE 93-95 Data Report. Faranda, F., Guglielmo, L., Povero, P., eds., S. Maria di Galeria: PNRA, pp. 307, 1997.
[30] E. P. McClain, W. G. Pichel, C. C. Walton,. Comparative performance of AVHRR-based Multichannel Sea Surface Temperature. Journal of Geophysical Research C **90**, 11587 (1985).
[31] R. M. Measures,. Laser Remote Sensing. Malabar: Krieger Publishing Company pp. 510, 1992.
[32] L. K. Medlin, J. Priddle, Polar marine diatoms (British Antarctic Survey, Natural Environment Research Council). Cambridge: Cambridge University Press, pp. 214, 1990.
[33] W. L. Miller, S. Johannessen, P. Kuhn, Proceedings of "Ocean Optics XV", October 16-20, 2000, Monaco, Monaco.
[34] D. M. Nelson, D. J. De Master, R. B. Dunbar, W. O. Smith Jr., Journal of Geophysical Research C **101**, 18519 (1996).
[35] J. E. O'Reilly, S. Maritorena, B. G. Mitchell, D. A. Siegel, K. L. Carder, S. A. Garver, M. Kahru, C. Mc Clain,. Ocean color chlorophyll algorithms for SeaWiFS. Journal of Geophysical Research C **103**, 24937 (1998).
[36] J. Priddle, G. Fryxell, Handbook of the common plankton diatoms of the Southern Ocean: Centrales except the genus Thalassiosira (British Antarctic Survey, Natural Environment Research Council). Cambridge: Cambridge University Press, pp. 159, 1985.
[37] V. Saggiomo, G. C. Carrada, O. Mangoni, D. Marino, M. Ribera D'Alcalà, in: Ross Sea Ecology. Italiantartide Expeditions (1987-1995). Faranda, F., Guglielmo, L., Ianora, A., eds. Berlin, Sprinter-Verlag, pp. 259, 2000.
[38] D. A. Siegel, S. Maritorena, N. B. Nelson, D. A. Hansell, M. Lorenzi-Kayser, Journal of Geophysical Research C **107**, 3228 (2002).
[39] W. O. Smith Jr, V. A. Asper, Antarctica, Deep-Sea Research II **48**, 137 (2001).
[40] W. O. Smith Jr., J. Marra, M. R. Hiscock, R. T. Barber, The seasonal cycle of phytoplankton biomass and primary productivity in the Ross Sea, Antarctica. Deep-Sea Research II **47**, 3119 (2000).
[41] W. O. Smith Jr., G. R. Di Tullio, A. R. Leventer, Journal of Geophysical Research C **101**, 18455 (1996).
[42] K. A. Steindinger, Dinoflagellates. In: Identifying Marine Diatoms and Dinoflagellates. Tomas, C. R., ed. San Diego: Academic Press, pp. 387, 1996.
[43] D. K. Stoecker, M. Putt, T. Moisan, Journal of the Marine Biological Association of the United Kingdom **75**, 815 (1995).
[44] C. Sweeney, D. A. Hansell, C. A. Carlson, L. A. Codispoti, L. I. Gordon, J. Marra, F. J. Millero, W. O. Smith, T. Takahashi, Biogeochemical regimes, net community production and carbon export in the Ross Sea, Antarctica. Deep-Sea Research II **47**, 3395 (2000).
[45] I. L. Thomas, R. W. Saunders, D. L. Croom, eds.. Applications of AVHRR data. Special issue of the International Journal of Remote Sensing **10**, 597 (1989).
[46] J. Throndsen,. The planktonic marine flagellates. In: Marine Phytoplankton: A Guide to Naked Flagellates and Coccolithophorids. Tomas, C. R., ed. San Diego: Academic Press, pp. 7, 1993.
[47] P. Tréguer, G. Jacques, Polar Biology **12**, 149 (1992).
[48] A. Zingone, G. Honsell, D. Marino, M. Montresor, G. Socal, Fitoplancton. In: Metodi nell'Ecologia del Plancton Marino. Innamorati, M., Ferrari, I., Marino, D., Ribera D'Alcalà, M. eds. Nova Thalassia **11**, 183 (1990).

*Corresponding author: fiorani@frascati.enea.it